Free energy barrier in the growth of sulfuric acid–ammonia and sulfuric acid–dimethylamine clusters

T. Olenius, O. Kupiainen-Määttä, I. K. Ortega, T. Kurtén, and H. Vehkamäki

Citation: J. Chem. Phys. **139**, 084312 (2013); doi: 10.1063/1.4819024
View online: http://dx.doi.org/10.1063/1.4819024
View Table of Contents: http://jcp.aip.org/resource/1/JCPSA6/v139/i8
Published by the AIP Publishing LLC.

Free energy barrier in the growth of sulfuric acid–ammonia and sulfuric acid–dimethylamine clusters

T. Olenius,[1,a)] O. Kupiainen-Määttä,[1] I. K. Ortega,[1] T. Kurtén,[2] and H. Vehkamäki[1]
[1]*Department of Physics, University of Helsinki, FIN-00014 Helsinki, Finland*
[2]*Department of Chemistry, University of Helsinki, FIN-00014 Helsinki, Finland*

(Received 22 April 2013; accepted 8 August 2013; published online 29 August 2013)

The first step in atmospheric new particle formation involves the aggregation of gas phase molecules into small molecular clusters that can grow by colliding with gas molecules and each other. In this work we used first principles quantum chemistry combined with a dynamic model to study the steady-state kinetics of sets of small clusters consisting of sulfuric acid and ammonia or sulfuric acid and dimethylamine molecules. Both sets were studied with and without electrically charged clusters. We show the main clustering pathways in the simulated systems together with the quantum chemical Gibbs free energies of formation of the growing clusters. In the sulfuric acid–ammonia system, the major growth pathways exhibit free energy barriers, whereas in the acid–dimethylamine system the growth occurs mainly via barrierless condensation. When ions are present, charged clusters contribute significantly to the growth in the acid–ammonia system. For dimethylamine the role of ions is minor, except at very low acid concentration, and the growing clusters are electrically neutral.
 [http://dx.doi.org/10.1063/1.4819024]

I. INTRODUCTION

Atmospheric aerosol particles are known to affect the global climate both directly by scattering and absorbing radiation and indirectly by acting as cloud condensation nuclei. The indirect effect is currently the largest single source of uncertainty in modeling and predicting the radiative forcing (IPCC[1]). Significant fractions of the aerosol particles and the cloud condensation nuclei have been estimated to originate from atmospheric gas-to-particle phase transition (Merikanto *et al.*,[2] Pierce and Adams,[3] and Kerminen *et al.*[4]) that starts with the clustering of individual gas phase molecules and proceeds by the clusters growing by collisions with gas molecules and each other. However, the molecular-level mechanisms and the compounds involved in the initial steps of the process still remain uncertain. Sulfuric acid has been shown to be the key compound in atmospheric particle formation (see, for example, Kuang *et al.*[5] and Sihto *et al.*[6]), but is not alone able to explain the formation rates observed in the troposphere. Instead, other atmospherically relevant species, such as bases and organic compounds, as well as ions, have been proposed to enhance the formation and growth of sulfuric acid-containing particles (see, for example, Zhang *et al.*,[7] Zhang *et al.*,[8] and Hou *et al.*[9]), out of which base compounds, most importantly ammonia and amines, seem to be promising candidates to take part in the first steps of cluster formation. Ammonia and dimethylamine have been theoretically shown to be capable of stabilizing sulfuric acid clusters (Kurtén *et al.*[10] and Loukonen *et al.*[11]). In experimental studies, ammonia has been observed to increase particle formation rates to some extent (Kirkby *et al.*[12]) and dimethylamine has been detected in molecular clusters in field measurements during new particle formation events (Kulmala *et al.*[13]).

A major challenge involved in studying the formation of the initial molecular clusters has been the lack of experimental methods capable of observing the smallest clusters and determining their chemical composition. Development of measurement instruments now permits the detection and chemical characterization of charged clusters down to single molecules (Junninen *et al.*[14]) and the detection of electrically neutral clusters down to a few molecules (Kulmala *et al.*[13]). On the other hand, the chemical characterization of neutral clusters still requires the clusters to be first charged, which may affect their composition (Kurtén *et al.*[15]). Given that atmospheric particle formation in the boundary layer may proceed for the most part via neutral pathways (Kulmala *et al.*[13] and Kulmala *et al.*[16]), theoretical methods are needed to give insights into processes involving both charged and neutral molecular clusters.

An essential question concerning the cluster growth is the existence of an energy barrier, and the size and chemical composition of the critical cluster if such a barrier exists. The critical cluster has equal probabilities to grow and to decay; clusters that are smaller than the critical size tend to shrink by evaporation, and clusters that are larger than the critical size tend to grow by condensation. In the classical liquid droplet model for a one-component system the energy barrier appears as a single maximum in the Gibbs free energy of formation located at the critical cluster size. For a multicomponent system the critical cluster is found at the saddle point, which is a maximum in one direction and a minimum in the other directions. A widely used method to estimate the composition of the critical cluster is the first nucleation theorem in its most readily applicable form, according to which the slope of the logarithm of the particle formation rate as a function of the

a)Author to whom correspondence should be addressed. Electronic mail: tinja.olenius@helsinki.fi

logarithm of the concentration of any component in the system gives the number of molecules of the component in question in the critical cluster. In general, the nucleation theorem is not simply a product of the classical liquid droplet model, but valid independent of how the cluster energies are obtained. However, the true free energy surface may be more complex than is assumed in the bulk droplet model, and the model is certainly not a reasonable approximation for clusters consisting of a few molecules. Instead, currently the most accurate theoretical method to study the properties of small clusters is quantum chemistry.

Quantum chemical calculations can be used to obtain the electronic energies and thermochemical parameters, such as the Gibbs free energies of formation, of molecular clusters (see, for example, Kurtén *et al.*,[10] Loukonen *et al.*,[11] Nadykto *et al.*,[17] Temelso *et al.*,[18] and Leverentz *et al.*[19]). Even though different quantum chemical methods may give quantitatively different results, they predict qualitatively similar trends for instance in terms of the composition of the most stable clusters, as they essentially model the fundamental chemistry of the molecules. The formation free energies can give information on the relative stability of the clusters, but to study the kinetics of a cluster population, the birth-death equations describing the formation and destruction of the clusters by collisions and evaporations have to be solved. Modeling cluster kinetics has been the topic of a number of studies on atmospheric new particle formation (see, for example, Schenter *et al.*,[20] Kathmann *et al.*,[21] Yu,[22] Yu,[23] and McGrath *et al.*[24] and references therein). Different approaches have been utilized to determine the collision and evaporation rate coefficients, but, they are in general assumed to be related via the detailed balance, that is, the equilibrium cluster distribution, which is in turn determined by the formation free energies.

In this study we used evaporation rates based on quantum chemical formation free energies together with collision rates obtained from the kinetic gas theory in a dynamic model. We studied two-component sulfuric acid–base systems, where the base is either ammonia or dimethylamine (DMA). We present the main clustering pathways in these systems and show how the growth occurs with respect to the corresponding formation free energy surfaces, and find essential differences between the systems with ammonia and DMA.

II. METHODS

A. Gibbs free energy of formation

The Gibbs free energies of formation were calculated using a quantum chemical multi-step method (Ortega *et al.*[25]) that combines geometry optimizations and frequency calculations performed with the Gaussian09 program (Frisch *et al.*[26]) using the B3LYP functional (Becke[27]) and a CBSB7 basis set (Montgomery *et al.*[28]) with single point energy calculations performed with the TURBOMOLE program (Ahlrichs *et al.*[29]) using the RI-CC2 method (Hättig and Weigend[30]) and an aug-cc-pV(T+d)Z basis set (Dunning *et al.*[31]) and are given in Table SI in the supplementary material.[32] In practice the thermal contributions to the free energies at different temperatures were calculated from vibrational frequencies and rotational constants obtained from the quantum chemical calculations. The formation free energies ΔG_{ref} are originally calculated at reference pressure P_{ref} of 1 atm and can be converted to actual vapor pressures of the components as (for a detailed derivation, see, for example, Vehkamäki[33] and references therein)

$$\Delta G(P_1, P_2, \ldots, P_n) = \Delta G_{\mathrm{ref}} - k_{\mathrm{B}} T \sum_{i=1}^{n} N_i \ln\left(\frac{P_i}{P_{\mathrm{ref}}}\right), \quad (1)$$

where n is the number of components in the cluster, N_i is the number of molecules of type i in the cluster and P_i is the partial pressure of component i in vapor phase, T is the temperature, and k_{B} is the Boltzmann constant. For charged clusters, N_i is taken to be the number of electrically neutral molecules, which is consistent with the conventions of ion-induced nucleation theory (Yue and Chan[34]). It should be noted that the quantum chemical formation free energies are calculated with respect to neutral and charged monomers, and therefore they are zero for all monomers regardless of the charge. On the other hand, as only electrically neutral molecules are considered in the conversion (Eq. (1)), the formation free energies of charged monomers remain zero, while the converted formation energies of neutral monomers are non-zero. It should also be noted that the Gibbs free energies of formation, as well as other thermochemical data, are normally reported at some reference pressure, but the quantity given by Eq. (1) is the actual formation free energy at the given monomer vapor pressures, which is used to determine the free energy surface and appears for example in the exponential of the classical nucleation theory expression for the nucleation rate.

B. ACDC model

We used the Atmospheric Cluster Dynamics Code (ACDC; McGrath *et al.*[24]) to solve the steady state of the cluster distribution. The code generates the time derivatives of the concentrations of all clusters and uses the Matlab ode15s routine for differential equations to simulate the time-dependent cluster concentrations. The time derivatives, also called the birth-death equations, include source terms from collisions of smaller clusters and evaporations from larger clusters, and sink terms from collisions with other clusters and evaporations into smaller clusters. The birth-death equation for each cluster can be written as

$$\frac{dC_i}{dt} = \frac{1}{2}\sum_{j<i} \beta_{j,(i-j)} C_j C_{i-j} + \sum_j \gamma_{(i+j)\to i,j} C_{i+j} - \sum_j \beta_{i,j} C_i C_j - \frac{1}{2}\sum_{j<i} \gamma_{i\to j,(i-j)} + Q_i - S_i, \quad (2)$$

where C_i is the concentration of cluster i, $\beta_{i,j}$ is the collision coefficient of clusters i and j, and $\gamma_{k\to i,j}$ is the evaporation coefficient of cluster k evaporating into clusters i and j. Q_i and S_i are possible additional source and sink terms, respectively. In this study we used an additional loss term corresponding to the coagulation of the clusters onto pre-existing larger particles.

If both electrically neutral and negatively and positively charged clusters are included in the simulation, the birth-death

equations include also source and sink terms from the ionization and recombination. All clusters containing sulfuric acid can get negatively ionized by losing one proton (that is, one sulfuric acid molecule is converted into a bisulfate ion), and correspondingly all base-containing clusters can get positively ionized by gaining one proton. For example, for a neutral cluster that can get negatively ionized the additional terms are

$$\left.\frac{dC_i}{dt}\right|_{\text{ionization,recombination}} = -\beta_{i,\text{ion}_{\text{neg.}}} C_i C_{\text{ion}_{\text{neg.}}} + \alpha_{\text{rec}} C_{i_{\text{neg.}}} C_{\text{ion}_{\text{pos.}}}, \tag{3}$$

where subscript $i_{\text{neg.}}$ refers to the negatively charged cluster with the same composition as the neutral cluster i, "$\text{ion}_{\text{neg.}}$" and "$\text{ion}_{\text{pos.}}$" refer to negative and positive generic ions, respectively, and α_{rec} is the recombination rate coefficient of positive and negative ions. Naturally, the terms in Eq. (3) appear in the equation for the negatively charged cluster $i_{\text{neg.}}$ with opposite signs, and corresponding terms can be written for positive ionization. The generic ionizing species are introduced into the system as constant source terms and are assumed to have the masses of O_2^- (32.00 u) and H_3O^+ (19.02 u) ions. The concentrations of the generic ions are also governed by birth-death equations that include the source term, collisions with all clusters that can get charged by the ion, recombinations with charged clusters and generic ions of the opposite sign, and the coagulation sink.

Collision rates between neutral clusters are obtained from the kinetic gas theory assuming a sticking factor of unity:

$$\beta_{i,j} = \left(\frac{3}{4\pi}\right)^{1/6} \left[6k_{\text{B}}T\left(\frac{1}{m_i}+\frac{1}{m_j}\right)\right]^{1/2} \left(V_i^{1/3}+V_j^{1/3}\right)^2, \tag{4}$$

where m_i and V_i are the mass and mass volume of cluster i, respectively. According to recent experimental findings (Bzdek *et al.*[35]), the collision rates may be decreased by energy barriers related to the collision processes, but in the absence of numerical values for the barrier heights we continued to use hard-sphere collision rates. If numerical values become available, they can easily be implemented in the ACDC framework (see Sec. III D). For collision rates between neutral and charged clusters we used an expression dependent on the polarizability and the dipole moment of the neutral cluster (Su and Bowers,[36] see also Kupiainen *et al.*[37]):

$$\beta_{i,j} = 2\pi Ze\left(\frac{1}{m_i}+\frac{1}{m_j}\right)^{1/2}\left[\alpha_j^{1/2} + c\mu_j\left(\frac{2}{\pi k_{\text{B}}T}\right)^{1/2}\right], \tag{5}$$

where Ze is the charge of the ionic cluster i, α_j, and μ_j are the polarizability and the dipole moment of the neutral cluster j, and c is a numerical scaling factor, for which the value of 0.15 was used as recommended by Su and Bowers.[36] The polarizabilities and dipole moments of all neutral clusters can be found in Table SII in the supplementary material.[32] The recombination coefficient of positive and negative ions (in all collisions involving charged molecular clusters and/or generic ions) was taken to be 1.6×10^{-6} cm^{-3} s^{-1} (Israël[38] and Bates[39]). Ions (charged clusters and/or generic ions) of the same polarity are not allowed to collide with each other because of electrostatic repulsion.

Evaporation rates were derived from the Gibbs free energies of formation of the clusters as described by Ortega *et al.*:[25]

$$\gamma_{(i+j)\to i,j} = \beta_{i,j}\frac{P_{\text{ref}}}{k_{\text{B}}T}\exp\left(\frac{\Delta G_{\text{ref},i+j}-\Delta G_{\text{ref},i}-\Delta G_{\text{ref},j}}{k_{\text{B}}T}\right), \tag{6}$$

where $\Delta G_{\text{ref},i}$ is the Gibbs free energy of formation of cluster i, and P_{ref} is the reference pressure where the free energies have been calculated. It should be noted that here the formation free energies need not be converted to actual monomer vapor pressures as in Eq. (1), since the conversion terms would cancel out in Eq. (6).

Clusters are allowed to grow out of the simulated system according to boundary conditions that are based on the composition of the outgrowing clusters and are discussed in more detail in Sec. II C 1. When a collision results in a cluster that is outside the system but does not satisfy the boundary conditions, it is forced back to the nearest boundary of the simulation box by evaporating molecules out of it. The evaporated molecules are returned to the simulation as free monomers (note that this is a new feature in the model compared to McGrath *et al.*[24]).

ACDC enables monitoring of the cluster concentrations and the fluxes between the clusters and out of the simulated system. The net flux between two clusters is defined as collisions minus evaporations in the case of clusters colliding and fragmenting, or ionizations minus recombinations in the case of clusters getting charged and neutralized. In this study we first examined which clusters mainly contribute to the flux out of the system, and then studied how these clusters are formed by tracing back the main flux chains down to monomers.

C. Simulated systems

In principle the simulated system is an "$m \times m$ box," where m is the maximum number of sulfuric acid (H_2SO_4) and base molecules in the clusters, and the base molecules can be either ammonia (NH_3) or DMA ($(CH_3)_2NH$). For the acid–DMA system, the size of the simulation box is 4×4; for the acid–ammonia system, the set was extended to 5×5 for reasons discussed in Sec. III B. For both bases, the simulations were performed including (1) only electrically neutral clusters and (2) both neutral clusters and negatively and positively charged cluster ions. The ionic molecules in negatively and positively charged clusters are a bisulfate ion (HSO_4^-) and a base molecule containing an extra proton (H^+), respectively. These are the charged molecules that are not considered in Eq. (1). The clusters do not contain water molecules, as quantum chemical data for the hydrates of the set of clusters studied in this work are not yet available. While water can be expected to somewhat stabilize acid–ammonia and especially pure acid clusters, it does not have a significant effect on the stability of acid–DMA clusters which are extremely stable. As the dominant interaction in the binding of the clusters is that between acid and ammonia or DMA, which are stronger bases than water, the qualitative steady-state distributions and growth routes are unlikely to be affected by hydration.

TABLE I. Schematic diagram of clusters explicitly included in the simulations. Rows indicate the number of acid molecules and columns indicate the number of base molecules in the cluster. N and D refer to the systems with ammonia and DMA, respectively.

(a) Electrically neutral clusters

	0 bases	1 base	2 bases	3 bases	4 bases	5 bases
0 acids		N, D	N, D	N, D	N, D	
H_2SO_4	N, D	N, D	N, D	N, D	N, D	
$(H_2SO_4)_2$	N, D	N, D	N, D	N, D	N, D	
$(H_2SO_4)_3$	N, D	N, D	N, D	N, D	N, D	
$(H_2SO_4)_4$	N, D	N, D	N, D	N, D	N, D	N
$(H_2SO_4)_5$	N	N	N	N	N	N

(b) Negatively charged clusters

	0 bases	1 base	2 bases	3 bases	4 bases	5 bases
HSO_4^-	N, D	N, D				
$(H_2SO_4)\cdot HSO_4^-$	N, D	N, D	D			
$(H_2SO_4)_2\cdot HSO_4^-$	N, D	N, D	N, D	D		
$(H_2SO_4)_3\cdot HSO_4^-$	N, D	N, D	N, D	N, D	D	
$(H_2SO_4)_4\cdot HSO_4^-$	N	N	N	N	N	

(c) Positively charged clusters

	0 bases	1 base + H^+	2 bases + H^+	3 bases + H^+	4 bases + H^+	5 bases + H^+
0 acids		N, D	N, D	N, D		
H_2SO_4		N, D	N, D	N, D		
$(H_2SO_4)_2$		N, D	N, D	N, D	N, D	
$(H_2SO_4)_3$			N	N, D	N, D	N
$(H_2SO_4)_4$				N, D	N, D	N
$(H_2SO_4)_5$						N

To avoid unnecessary computational costs, the set of clusters was restricted based on the relative stability of the clusters, and therefore clusters that could be predicted to be highly unstable were left out of the simulation. The negative cluster ions were defined as unstable if the number of base molecules in the cluster is equal to or higher than that of acid molecules, and similarly the positive cluster ions are unstable if they contain more acid than base molecules. Also some neutral and positive clusters that have a very high base:acid ratio were omitted. A complete list of clusters included in the simulations is presented in Table I. Sulfuric acid, ammonia, and DMA molecules are abbreviated with A, N, and D, respectively. Clusters are named according to the abbreviations followed by the number of molecules of the compound, and negative and positive charges are denoted with minus and plus signs, respectively. For example, a neutral cluster with two acid and two ammonia molecules is denoted with A_2N_2, and negative and positive cluster ions with the same composition are denoted with $(A_2N_2)^-$ and $(A_2N_2)^+$.

1. Boundary conditions

As the clusters that are allowed to leave the system are assumed to be stable enough not to evaporate back immediately, the boundary conditions require the outgrowing clusters to have a favorable composition. Neutral clusters that have the lowest evaporation rates and highest concentrations in the simulations have approximately equal numbers of acid and base molecules (in the case of ammonia, the number of acid molecules in the most stable clusters is mostly equal to or one higher than the number of base molecules, whereas for DMA the number of acids is mostly equal to or, for larger clusters, one lower than the number of bases; see also Ortega *et al.*[25]). Therefore, for ammonia, neutral clusters containing at least $m + 1$ acid and m base molecules are allowed to leave the $m \times m$ simulation box. For DMA, outgrowing clusters can have either $m + 1$ acids and m bases, or m acids and $m + 1$ bases. The second condition is based on the following reasoning: as the simulations showed that A_3D_4 does not in practice evaporate ($\gamma_{A_3D_4} = 1.93 \times 10^{-3}$ s^{-1} at $T = 5\,^\circ$C), we calculated also the evaporation rate of A_4D_5 (although it is outside the default 4×4 box) and found it to be even lower than the evaporation rate of A_3D_4 ($\gamma_{A_4D_5} = 6.73 \times 10^{-6}$ s^{-1} at $T = 5\,^\circ$C). Thus A_4D_5 clusters are allowed to grow out of the system.

In systems with ions, the outgrowing negative clusters are required to have at least $m + 1$ acids, including the bisulfate ion, and one base. The base molecule is required since negative clusters with five or six acids and no bases are not stable. The composition of the most stable positive cluster ions depends on the base. For ammonia, the number of base molecules is typically one higher or equal to the number of acids, and for DMA, the number of bases is one or two higher than the number of acids. Therefore the outgrowing positive clusters must have at least m acids and $m + 1$ bases for ammonia, and $m - 1$ acids and $m + 1$ bases for DMA. The condition for positive DMA clusters is based on reasoning similar to what was applied for the conditions of neutral acid–DMA clusters: evaporation of $(A_2D_4)^+$ clusters is negligible ($\gamma_{(A_2D_4)^+} = 3.53 \times 10^{-4}$ s^{-1} at $T = 5\,^\circ$C), and therefore it

is reasonable to assume the $(A_3D_5)^+$ cluster to be stable as well.

D. Simulated conditions

We performed the simulations using sulfuric acid and base concentrations, a temperature, and an ion production rate relevant to atmospheric conditions. We used constant concentrations for the ammonia and DMA monomers. Gas-phase sulfuric acid concentration is normally measured with the Chemical Ionization Mass Spectrometer (CIMS; see, for example, Berresheim *et al.*[40] and Petäjä *et al.*[41]) which can also detect acid molecules clustered with base molecules as pure acid monomers (Kurtén *et al.*[15]). Thus the acid concentration $[H_2SO_4]$ was defined as the total concentration of all neutral clusters containing one acid and any number of base molecules. It must be noted here that the actual monomer concentration of acid has to be used in the conversion of ΔG_{ref} in Eq. (1). Therefore we first ran the simulations with $[H_2SO_4]$ defined as above, and used the actual steady-state acid monomer concentration obtained from the simulations in the conversion to obtain the corresponding formation free energy surface.

The simulations were mostly run at 5 °C, with additional test runs performed at 15 °C to study the effect of temperature. The temperature of 5 °C was chosen as it corresponds to typical spring-time conditions at a boreal forest site in Hyytiälä, Finland, where many field measurements of new particle formation have been carried out (see, for example, Manninen *et al.*[42] and Manninen *et al.*[43]). The sulfuric acid concentration was set to 10^5, 10^6, and 10^7 cm^{-3}, a range relevant to atmospheric particle formation (Kuang *et al.*[5] and Kerminen *et al.*[44]). Atmospheric base concentrations are not as well known, and we chose to use for ammonia 50, 100, and 500 ppt (corresponding to 1.3×10^9 cm^{-3}, 2.6×10^9 cm^{-3}, and 1.3×10^{10} cm^{-3}) and for DMA 0.1, 1, and 10 ppt (corresponding to 2.6×10^6 cm^{-3}, 2.6×10^7 cm^{-3}, and 2.6×10^8 cm^{-3}), which are approximately of the same order of magnitude as what has been measured in boreal areas (Riipinen *et al.*[45] and Ge *et al.*[46]). Ammonia mixing ratios of this order have also been observed to enhance particle formation in the CLOUD chamber experiment (Kirkby *et al.*[12]). In the simulations including charged clusters, 3 ion pairs s^{-1} cm^{-3} was used for the ion production rate, corresponding to natural ionization by galactic cosmic rays (Kirkby *et al.*[12]). We used a constant coagulation sink coefficient of 2.6×10^{-3} s^{-1} as in Ref. 24, based on measurements in Hyytiälä (Dal Maso *et al.*[47]). The same value was used for both neutral and charged clusters (and the generic ions). In reality, coagulation losses might be enhanced for ions because of the electric charge, but we chose not to use any enhancement factor to ensure that the effect of ions is not underestimated. Additional test simulations were performed using an enhancement factor of 2 for the coagulation sink of ions.

III. RESULTS AND DISCUSSION

The clustering routes are presented as arrow plots on an acid–base grid, where the horizontal and vertical coordinates correspond to the numbers of acid and base molecules, respectively. The bisulfate ion in negative clusters is counted as one acid, and the positively charged base molecule in positive clusters is counted as one base. In case the flux into a cluster or out of the system has more than one major source, relative fractions of the total flux are marked in the figure. For clarity, only fluxes that are at least 10% of the total flux into the cluster (or out of the system) are shown in all the figures.

A. Sulfuric acid–ammonia system

Panel (a) in Figure 1 shows the growth pathways in the system of electrically neutral clusters consisting of sulfuric acid and ammonia at $T = 5$ °C, $[H_2SO_4] = 10^6$ cm^{-3} and $[NH_3] = 100$ ppt. The formation free energy surface and the ΔG of the outgrowing clusters as a function of growth step for the same conditions are presented in panels (b) and (c), respectively. Three main features can be observed in Fig. 1. First, the major growth occurs by addition of either one acid or one ammonia molecule and second, there are several free energy barriers along the growth pathways. Third, the clusters do not grow along the lowest energy pathway, but instead the kinetics of the system drives the clusters over higher barriers. For example, the AN cluster has lower formation energy than the acid dimer A_2, but nevertheless the growth from the acid monomer to the A_2N cluster (the formation energy of which is in practice equal to that of AN at 5 °C) occurs mainly via the dimer (panel (c) in Fig. 1). This is because the collision frequency of the dimer and the ammonia monomer is higher than that of the AN cluster and the acid monomer, as the ammonia concentration is much higher than the acid concentration and the collision coefficient β is larger.

The growth patterns are more diverse in the acid–ammonia system with ions (Figure 2): both neutral and charged clusters contribute to the outgoing fluxes, and moreover, the major fraction of the outgrowing neutral clusters are originally formed by recombination of charged clusters. The total formation rate of clusters outside the system is significantly enhanced by ions in all the studied conditions except at the high acid and ammonia concentrations $[H_2SO_4] = 10^7$ cm^{-3} with $[NH_3] = 500$ ppt, as shown in Table II. The cluster formation energies ΔG as a function of growth step for the system without ions and for the charged pathways in the system with ions at varying acid and ammonia concentrations are shown in Figures 3 and 4. According to the simulation results the measurable acid concentration (defined in Sec. II D) is the actual acid monomer concentration in the acid–ammonia system in all the studied conditions. The entirely neutral growth routes in the ionic system are qualitatively the same as in the system without ions, but at $[H_2SO_4] = 10^5$ cm^{-3} and 10^6 cm^{-3} recombination is a significant source of neutral clusters. The largest cluster on the major neutral pathway of which a notable fraction is formed from charged clusters is A_5N_3, formed in the collision of $(A_2N_3)^+$ and $(A_3)^-$. Figures 3 and 4 show that there are energy barriers also along the charged growth routes, both negative and positive.

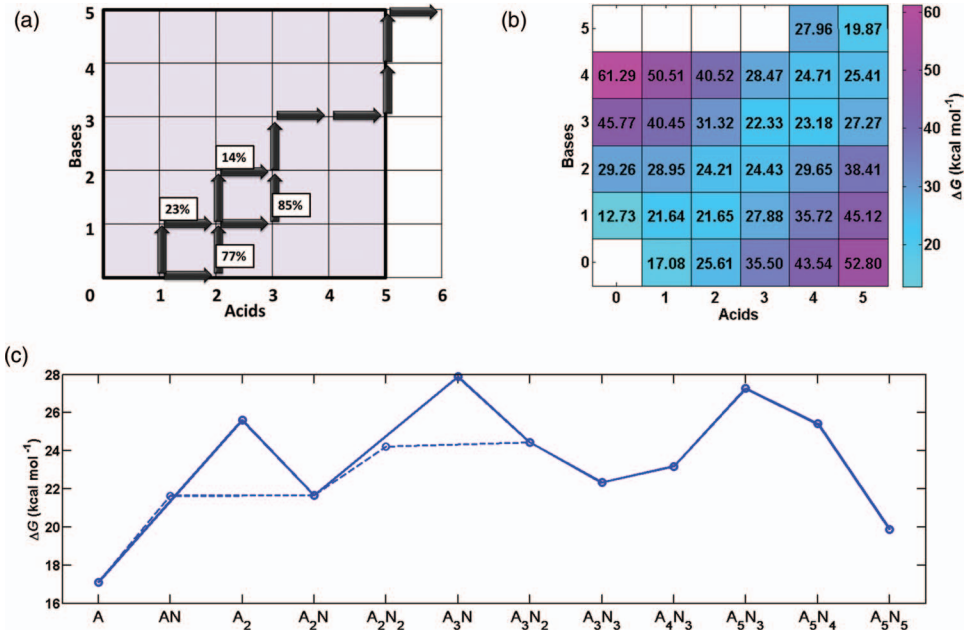

FIG. 1. Main clustering pathways and Gibbs free energies of formation of the clusters in the electrically neutral sulfuric acid–ammonia system at $T = 5\,^{\circ}\mathrm{C}$, $[H_2SO_4] = 10^6\ \mathrm{cm}^{-3}$, and $[NH_3] = 100$ ppt. Panel (a): Major routes leading out of the simulated system. Panel (b): Formation free energies of all clusters in the system. Panel (c): Formation free energy of the growing clusters as a function of growth step. Solid and dashed lines correspond to the major and minor fluxes, respectively.

The ΔG's of the clusters decrease as either the acid (Fig. 3) or ammonia (Fig. 4) concentration increases, with the decrease being larger for the larger clusters (Eq. (1)). The locations of the energy barriers nevertheless remain at the same cluster sizes, namely A_2, A_3N, and A_5N_3 for neutral clusters, $(A_4)^-$ and $(A_5N_2)^-$ for negative clusters, and $(A_2N_2)^+$, $(A_3N_3)^+$, $(A_4N_4)^+$, and $(A_5N_5)^+$ for positive clusters, but the location of the highest barrier may vary. The major growth in the conditions of Figs. 3 and 4 proceeds via the same pathways regardless of the acid and ammonia concentrations, but some minor routes may become more important as the concentrations are varied. As opposed to the neutral growth routes for which the first step increases the energy of the system, the first step along the charged growth routes (that is the formation of a negatively charged acid dimer or a positively charged ammonia dimer) is energetically very favorable. However, energy barriers appear along the following growth steps in all the studied conditions.

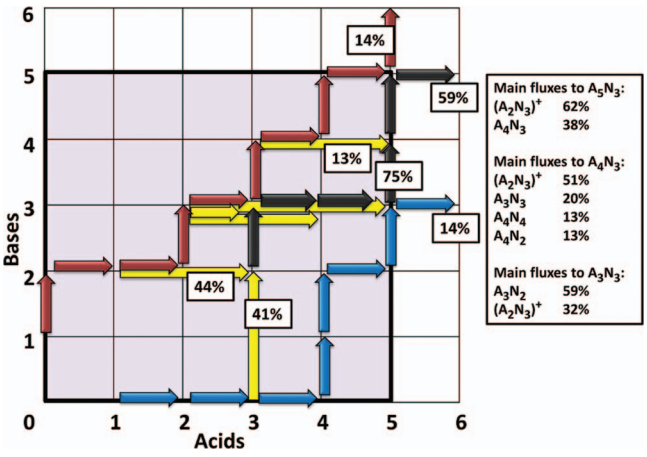

FIG. 2. Main clustering pathways in the sulfuric acid–ammonia system with ions at $T = 5\,^{\circ}\mathrm{C}$, $[H_2SO_4] = 10^6\ \mathrm{cm}^{-3}$, and $[NH_3] = 100$ ppt. Black, blue, and red arrows correspond to the growth pathways of electrically neutral, negatively charged and positively charged clusters, respectively. Formation of electrically neutral clusters in recombination of positive and negative clusters is denoted with yellow arrows. For figure clarity, some formation pathways (that are at least 10% of the flux into the cluster) are not drawn in the figure but are listed in the adjacent text box.

B. Sulfuric acid–DMA system

Figure 5 shows the growth pathways and ΔG's in the system of electrically neutral clusters consisting of sulfuric acid and DMA at $T = 5\,^{\circ}\mathrm{C}$, $[H_2SO_4] = 10^6\ \mathrm{cm}^{-3}$, and $[\mathrm{DMA}] = 1$ ppt. Cluster growth in the system with DMA is fundamentally different than in the system with ammonia in similar conditions (Fig. 1): collisions involving two clusters contribute significantly to the growth, and there are no energy barriers along the main growth pathways. As opposed to ammonia, the DMA molecule is capable of binding strongly already to a single sulfuric acid molecule. Consequently, a significant fraction of the acid molecules is clustered with a DMA molecule, which allows the clusters to grow also by colliding with the AD cluster. In addition, collisions with A_2D and A_2D_2 contribute to the cluster formation to some extent. The ΔG decreases monotonically along the main growth route out of the system (panel (c) in Fig. 5), partly because energy barriers are avoided by collisions with the small clusters rather than monomers.

Another important difference between the systems with ammonia and DMA is that ions do not significantly affect the growth pathways, or the absolute rate out of the simulated system, except at low acid and DMA concentrations $[H_2SO_4]$

TABLE II. Simulated particle formation rate (cm^{-3} s^{-1}) (the rate at which clusters grow out of the simulated system) for the sulfuric acid–ammonia and the sulfuric acid–DMA systems without and with ions at varying sulfuric acid and base concentrations.

		[NH_3]			[DMA]		
[H_2SO_4]		50 ppt	100 ppt	500 ppt	0.1 ppt	1 ppt	10 ppt
10^5 cm^{-3}	No ions	1.5×10^{-12}	7.9×10^{-12}	2.3×10^{-10}	8.6×10^{-6}	6.8×10^{-4}	1.2×10^{-3}
	With ions	3.7×10^{-9}	7.7×10^{-9}	4.1×10^{-8}	2.9×10^{-5}	1.1×10^{-3}	1.9×10^{-3}
10^6 cm^{-3}	No ions	1.1×10^{-6}	5.6×10^{-6}	1.5×10^{-4}	8.0×10^{-2}	5.0	9.0
	With ions	5.7×10^{-4}	1.0×10^{-3}	3.6×10^{-3}	9.7×10^{-2}	5.2	9.3
10^7 cm^{-3}	No ions	1.4×10^{-1}	5.9×10^{-1}	11.6	2.4×10^{2}	5.4×10^{3}	1.0×10^{4}
	With ions	7.8×10^{-1}	1.6	13.2	2.4×10^{2}	5.4×10^{3}	1.0×10^{4}

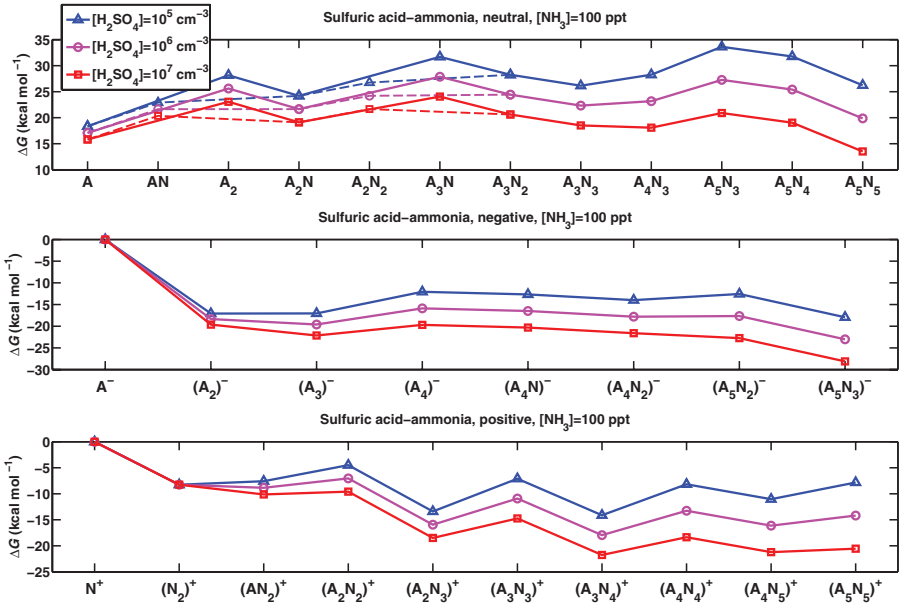

FIG. 3. Gibbs free energy of formation of the growing clusters as a function of growth step in the sulfuric acid–ammonia system for neutral, negative and positive growth routes at varying acid concentration at [NH_3] = 100 ppt and $T = 5\,^{\circ}C$. Solid and dashed lines correspond to the major and minor fluxes, respectively. Note the different scales of the y-axes.

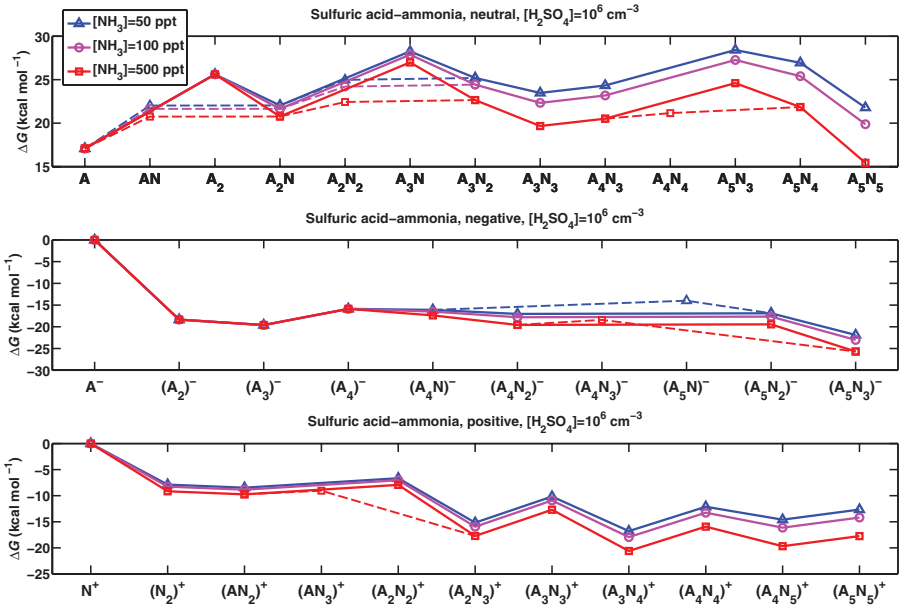

FIG. 4. Gibbs free energy of formation of the growing clusters as a function of growth step in the sulfuric acid–ammonia system for neutral, negative and positive growth routes at varying ammonia concentration at [H_2SO_4] = 10^6 cm^{-3} and $T = 5\,^{\circ}C$. Solid and dashed lines correspond to the major and minor fluxes, respectively. Note the different scales of the y-axes.

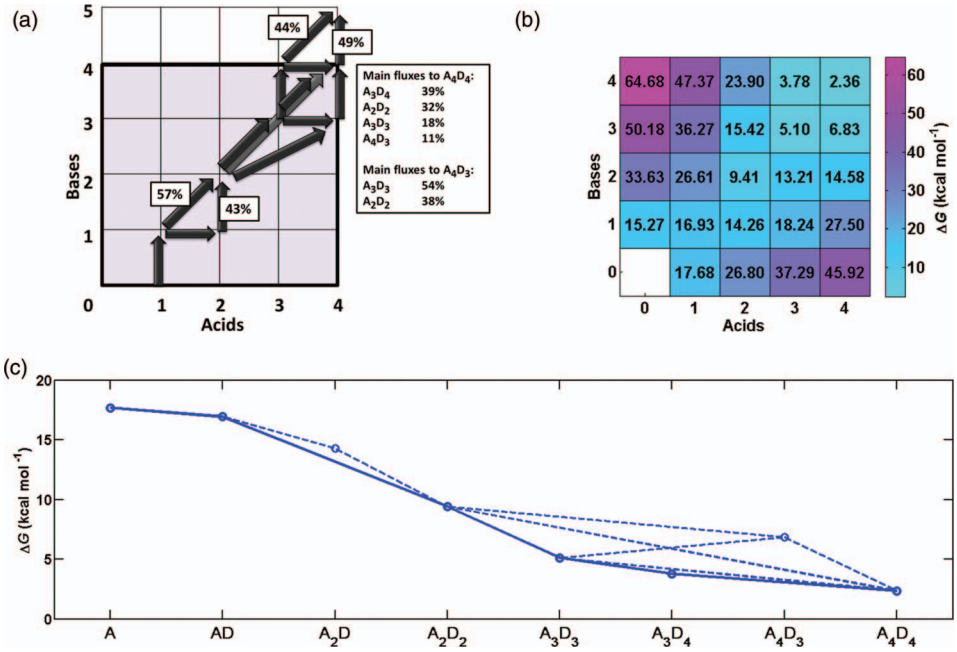

FIG. 5. Main clustering pathways and Gibbs free energies of formation of the clusters in the electrically neutral sulfuric acid–DMA system at $T = 5\,^{\circ}$C, $[H_2SO_4] = 10^6$ cm^{-3}, and [DMA] = 1 ppt. Panel (a): Major routes leading out of the simulated system. For figure clarity, the arrows that fall on top of each other are colored with different shades. Panel (b): Formation free energies of all clusters in the system. Panel (c): Formation free energy of the growing clusters as a function of growth step. Solid and dashed lines correspond to the major and minor fluxes, respectively.

$= 10^5$ cm^{-3} with [DMA] = 0.1, 1, and 10 ppt, and $[H_2SO_4]$ $= 10^6$ cm^{-3} with [DMA] = 0.1 ppt. In these conditions, the ions contribute mainly by growing out as positive clusters, but the flux out of the simulated system is anyhow very low, as presented in Table II. The presence of ions does not affect the formation routes of neutral clusters, except that a few percent of the boundary clusters (A_4D_4, A_3D_4, A_4D_3, and A_3D_3) are formed by recombination. Therefore the ΔG along the main neutral growth pathways is representative also for the system with ions. The main growth routes in the conditions where the contribution of ions is the most significant, $[H_2SO_4]$ $= 10^5$ cm^{-3} and [DMA] = 0.1 ppt, are shown in Figure 6. At $[H_2SO_4] = 10^6$ cm^{-3} and [DMA] = 1 ppt, the addition of ions increases the total rate out of the system by only 4% compared to the neutral system, and at $[H_2SO_4] = 10^7$ cm^{-3} the ions do not have practically any effect.

Figures 7 and 8 show the formation free energies of neutral sulfuric acid–DMA clusters along the major growth routes when either the acid or the DMA concentration is varied. Increasing the measurable acid concentration while keeping the

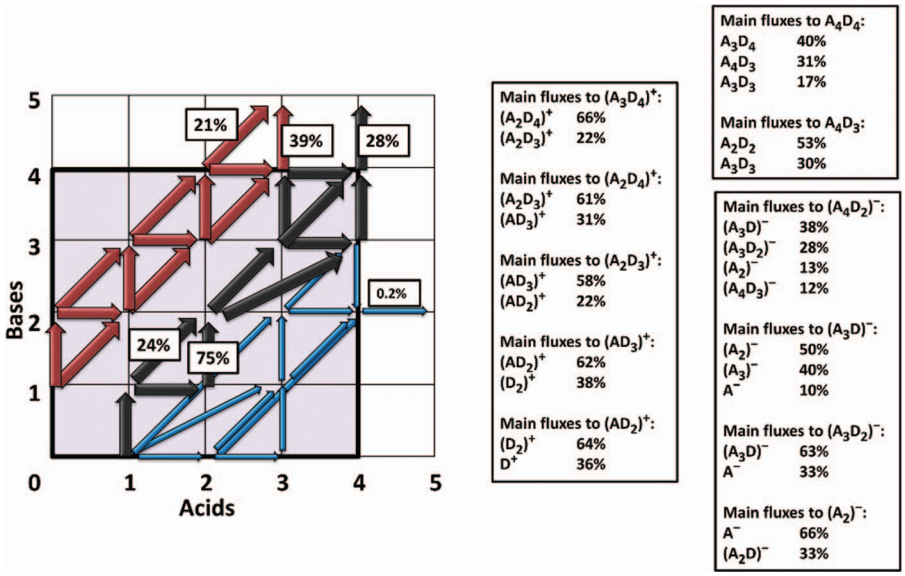

FIG. 6. Main clustering pathways in the sulfuric acid–DMA system with ions at $T = 5\,^{\circ}$C, $[H_2SO_4] = 10^5$ cm^{-3}, and [DMA] = 0.1 ppt. Black, blue, and red arrows correspond to the growth pathways of electrically neutral and negatively and positively charged clusters, respectively. Note that the negative pathways are insignificant, but are drawn in the figure for completeness.

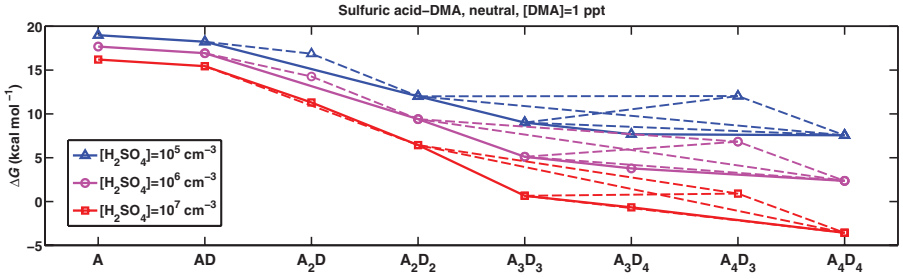

FIG. 7. Gibbs free energy of formation of the growing electrically neutral clusters as a function of growth step in the sulfuric acid–DMA system with or without ions at varying acid concentration at [DMA] = 1 ppt and $T = 5\,^{\circ}$C. Solid and dashed lines correspond to the major and minor fluxes, respectively. Note the different scales of the y-axes.

DMA concentration constant decreases all the ΔG's but does not have a significant effect on the slope of the curve (Fig. 7). If the DMA concentration is increased while the measurable acid concentration is kept constant, the true acid monomer concentration decreases as presented in Table III, because in the acid–DMA system the measurable acid concentration is effectively the sum of the A and AD concentrations. The decrease in the acid monomer concentration increases the ΔG value of the acid monomer (Eq. (1)), and the changes in the vapor monomer concentrations of both acid and DMA affect the ΔG's of the clusters containing both compounds. Thus the ΔG values do not systematically decrease, but rather the slope becomes steeper (Fig. 8). At the low DMA concentration [DMA] = 0.1 ppt, a low energy barrier is formed at the AD cluster. Varying the concentrations affects also the relative importance of different formation routes of some clusters to some extent; for example, the higher the DMA concentration, the higher the fraction of A_2D_2 clusters formed from two AD clusters instead of AD colliding first with one acid and then with one DMA molecule. The main outgoing fluxes correspond in most of the studied conditions to A_4D_4 colliding with D and A_3D_4 colliding with AD, with other notable fluxes being mainly due to collisions of A_4D_4, A_3D_4, A_4D_3, and A_3D_3 with A, AD, A_2D, and A_2D_2, in the way that the boundary conditions are satisfied.

The formation free energies of charged sulfuric acid–DMA clusters along the major growth routes in the conditions where the contribution of ions is significant are shown in Figure 9 (note that these conditions are different for the opposite polarities). It has to be noted that even in the studied conditions where the role of negatively charged growth pathways is the most prominent, $[H_2SO_4] = 10^6$ cm^{-3} and [DMA] = 0.1 ppt, the contribution of clusters growing out as negative ions to the total flux out of the system is a few percent. The negative clustering routes in these conditions are qualitatively similar to those at $[H_2SO_4] = 10^5$ cm^{-3} and [DMA] = 0.1 ppt (Fig. 6). It can be seen from Fig. 9 that the most important ionic routes are also barrierless. In the case of positive clusters, increasing the DMA concentration somewhat decreases the ΔG's and enables the main growth to proceed via collisions with AD clusters. As for the negative growth routes, the barrier at $(A_4)^-$ (Figs. 3 and 4) is avoided as DMA is capable of binding already to the negative trimer $(A_3)^-$ and stabilizing it, whereas ammonia can stabilize negative clusters containing at least four acid molecules (including the bisulfate ion). The negatively charged mono- and dimers A^- and $(A_2)^-$ are mainly formed by acid monomers being ionized and then growing further by addition of acid as in the acid–ammonia system, but minor fractions are formed by the small neutral clusters AD, A_2D, and A_2D_2 being ionized or colliding with a bisulfate ion. As the resulting negative clusters are not stable with the DMA molecules, the DMAs evaporate as indicated by the black arrows in Fig. 9. All the $(AD)^-$ and $(A_2D_2)^-$ clusters and a minor fraction of $(A_2D)^-$ clusters are formed by ionization of neutral clusters.

As stated in Sec. II C, the simulation box was extended from 4 × 4 to 5 × 5 for ammonia. This was done because the cluster formation energy increases along the main growth route towards the edge of the neutral 4 × 4 box (Fig. 1), and therefore it was not initially clear whether the clusters would enter a region of barrierless growth. The extension of the box, however, shows that the A_5N_5 cluster is very stable.

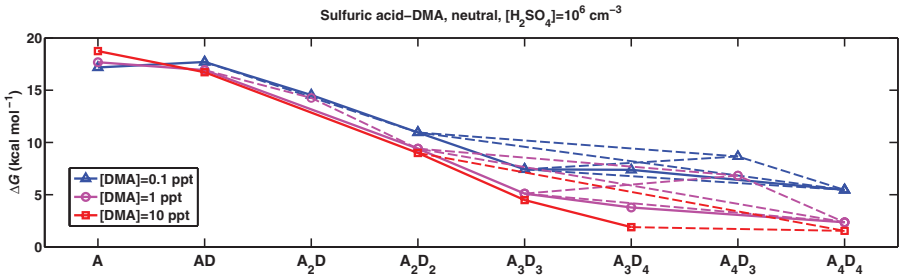

FIG. 8. Gibbs free energy of formation of the growing electrically neutral clusters as a function of growth step in the sulfuric acid–DMA system with or without ions at varying DMA concentration at $[H_2SO_4] = 10^6$ cm^{-3} and $T = 5\,^{\circ}$C. Solid and dashed lines correspond to the major and minor fluxes, respectively. Note the different scales of the y-axes.

TABLE III. Concentration of pure acid monomers (cm^{-3}) at varying DMA monomer concentration and measurable acid concentration [H_2SO_4], defined as the total concentration of electrically neutral clusters consisting of one acid and any number of DMA molecules.

	[DMA]		
[H_2SO_4]	0.1 ppt	1 ppt	10 ppt
10^5 cm^{-3}	8.3×10^4	3.2×10^4	4.6×10^3
10^6 cm^{-3}	8.4×10^5	3.4×10^5	4.9×10^4
10^7 cm^{-3}	9.0×10^6	5.0×10^6	9.3×10^5

Figures 7–9 indicate a clear decreasing trend for the ΔG along the most significant growth pathways in the system with DMA, and therefore the 4×4 box was considered to be sufficient.

C. Simulations at $T = 15\,^{\circ}C$

The results of the additional runs performed at a temperature of 15 °C are qualitatively similar to those at 5 °C. The enhancing effect of ions is more significant than at 5 °C for both bases, as the enhancement in the evaporation rates due to the temperature increase, caused by the $(k_B T)^{-1}$ factor in Eq. (6), is relatively larger for neutral clusters than for charged clusters which are more strongly bound because of the electrostatic forces. In the system with ammonia, the energy barriers appear at the same locations as in Figs. 3 and 4. For DMA, the ionic contribution was found to be negligible also at 15 °C, except at the low acid concentration [H_2SO_4] = 10^5 cm^{-3}, or at [H_2SO_4] = 10^6 cm^{-3} with [DMA] = 0.1 ppt. The ΔG decreases along the most significant growth routes, with the exception that low energy barriers appear at AD at [DMA] = 0.1 and 1 ppt and at A_3D_4 at [DMA] = 0.1 ppt.

D. Test simulations for error estimates

Major sources of uncertainties in the formation rates are the collision and evaporation coefficients. We used by default a sticking probability of unity in all collisions, which might be a better assumption for ammonia than for DMA. This is because the ammonia molecule is symmetrical and thus capable of forming hydrogen bonds equally on all sides, whereas the DMA molecule has on one side two methyl groups that cannot form bonds. On the other hand, the system with DMA is not sensitive to inaccuracies in the evaporation coefficients since the evaporation rates of clusters containing DMA are extremely low in any case. Therefore the error estimates were carried out by varying the evaporation coefficients in the case of ammonia, and the sticking factor in the case of DMA. It should be noted that the possible kinetic barriers related to the collisions discussed in Sec. II B will have exactly the same effect as the sticking factors. The method for calculating collision frequencies between neutral clusters and ions can also cause uncertainty; however, the expression used in this work has already been shown to give good results compared to experimental data in the study by Kupiainen *et al.*[37] Furthermore, the inaccuracy of the collision coefficients is unlikely to be more than a factor of two or so (Ortega *et al.*[25]), which is much smaller than for evaporation rates and sticking factors.

In the acid–ammonia system, the evaporation rates were scaled by changing the Gibbs free energies of all the clusters by ±1 kcal mol^{-1}, which is the estimated uncertainty in the quantum chemical results. While the scaling decreases or increases the total flux out of the system, the clustering pathways remain qualitatively similar. The change in the formation rate is relatively larger in the electrically neutral system. The role of charged clusters is still significant in the ionic system, with the exception that the contribution of ions is very minor at [H_2SO_4] = 10^7 cm^{-3} in the case where all clusters are stabilized by 1 kcal mol^{-1}. Recombination processes

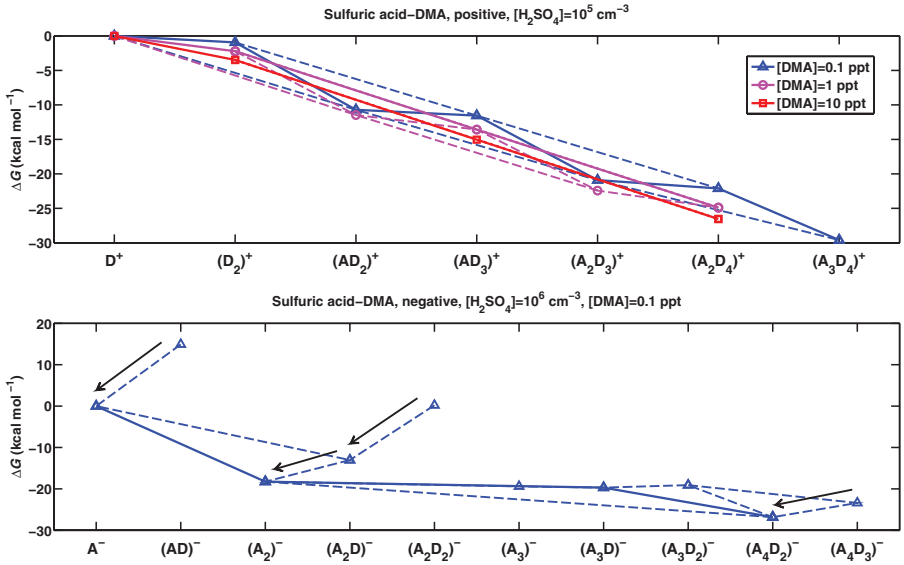

FIG. 9. Gibbs free energy of formation of the charged growing clusters as a function of growth step in the sulfuric acid–DMA system with ions in the conditions where the contribution of charged clusters is significant at $T = 5\,^{\circ}C$. Solid and dashed lines correspond to the major and minor fluxes, respectively. Minor fractions of some of the larger negatively charged clusters are formed by neutral clusters colliding with a bisulfate ion, but for clarity the corresponding lines are not included in the figure. The arrows indicate evaporation from larger sizes. Note the different scales of the y-axes.

become more or less significant when the clusters are destabilized or stabilized, respectively.

In the acid–DMA system, the sticking factor in all collisions between two neutral clusters of which at least one contains DMA was decreased to 0.5, and the sticking factor in collisions involving charged clusters was retained at unity. As can be predicted, this promotes the relative importance of ions in all the studied conditions. The effect of ions is the most significant in the same conditions as before. At $[H_2SO_4] = 10^5$ cm^{-3} with [DMA] = 0.1 ppt, the addition of ions results in a 50-fold increase in the flux out of the system, and at $[H_2SO_4] = 10^5$ cm^{-3} with [DMA] = 1 and 10 ppt, and $[H_2SO_4] = 10^6$ cm^{-3} with [DMA] = 0.1 ppt, the increase is approximately 5-fold. In the other conditions, neutral pathways still dominate. Addition of ions increases the outgoing flux by 31% at $[H_2SO_4] = 10^6$ cm^{-3} with [DMA] = 1 ppt, and by 20% at $[H_2SO_4] = 10^6$ cm^{-3} with [DMA] = 10 ppt. At $[H_2SO_4] = 10^7$ cm^{-3} the contribution of ions is negligible. The formation pathways are not qualitatively affected.

In order to ensure that the effect of ions is not overestimated by too small loss terms, additional test runs were performed with the coagulation sink of charged clusters and generic ions enhanced by a factor of 2. In the acid–ammonia system, this expectedly decreases the total formation rate and the fraction of neutral clusters formed in recombination, but the contribution of ions remains nevertheless significant.

IV. SUMMARY AND CONCLUSIONS

We used quantum chemical formation free energy data for molecular clusters consisting of sulfuric acid and either ammonia or dimethylamine (DMA) molecules in a dynamic model and studied the steady-state fluxes leading out of the simulated system in atmospherically relevant conditions at a temperature of 5 °C. We converted the quantum chemical Gibbs free energies of formation of the growing clusters ΔG to the acid and base concentrations used in the simulations and studied the formation free energy profiles of the cluster growth in the sulfuric acid–ammonia and sulfuric acid–DMA systems, both with and without charged clusters.

In the sulfuric acid–ammonia system without ions, the growth proceeds by collisions with single acid or ammonia molecules. In the system with both neutral and charged clusters, charged clusters contribute to the major formation routes both by growing out via collisions with neutral monomers and by forming neutral clusters via recombination. The ΔG along the main growth pathways exhibits energy barriers in both the electrically neutral system and the system with ions.

The growth pathways in the acid–DMA system include significant contributions from collisions with small clusters that are relatively abundant in the system, as the DMA molecule binds strongly to sulfuric acid. This should be considered in condensation models, as well as in the interpretation of sulfuric acid concentration measurements performed with the CIMS (Chemical Ionization Mass Spectrometer). The main growth occurs via electrically neutral pathways also in the presence of ions, except at very low acid concentration, where the contribution of positively charged clusters is prominent. Each growth step along the main clustering routes, both neutral and charged, decreases the Gibbs free energy of the growing clusters, except for the neutral pathways at very low DMA concentrations. Thus there is no critical cluster in the acid–DMA system in conditions typical to the lower atmosphere, and in this case conclusions of the critical cluster composition based on the slope of the observed particle formation rate are meaningless.

ACKNOWLEDGMENTS

We thank ERC Projects Nos. 257360-MOCAPAF and 27463-ATMNUCLE, Vilho, Yrjö and Kalle Väisälä Foundation and Academy of Finland LASTU program Project No. 135054 for funding, and CSC–IT Center for Science in Espoo, Finland for computing time.

[1] IPCC, The Intergovernmental Panel on Climate Change, *Climate Change 2007: The Physical Science Basis* (Cambridge University Press, New York, 2007).
[2] J. Merikanto, D. V. Spracklen, G. W. Mann, S. J. Pickering, and K. S. Carslaw, Atmos. Chem. Phys. **9**, 8601 (2009).
[3] J. R. Pierce and P. J. Adams, Atmos. Chem. Phys. **9**, 1339 (2009).
[4] V.-M. Kerminen, M. Paramonov, T. Anttila, I. Riipinen, C. Fountoukis, H. Korhonen, E. Asmi, L. Laakso, H. Lihavainen, E. Swietlicki, B. Svenningsson, A. Asmi, S. N. Pandis, M. Kulmala, and T. Petäjä, Atmos. Chem. Phys. **12**, 12037 (2012).
[5] C. Kuang, P. H. McMurry, A. V. McCormick, and F. L. Eisele, J. Geophys. Res. **113**, D10209, doi:10.1029/2007JD009253 (2008).
[6] S.-L. Sihto, M. Kulmala, V.-M. Kerminen, M. Dal Maso, T. Petäjä, I. Riipinen, H. Korhonen, F. Arnold, R. Janson, M. Boy, A. Laaksonen, and K. E. J. Lehtinen, Atmos. Chem. Phys. **6**, 4079 (2006).
[7] R. Zhang, I. Suh, J. Zhao, D. Zhang, E. C. Fortner, X. Tie, L. T. Molina, and M. J. Molina, Science **304**, 1487 (2004).
[8] R. Zhang, A. Khalizov, L. Wang, M. Hu, and W. Xu, Chem. Rev. **112**, 1957 (2012).
[9] G.-L. Hou, W. Lin, S. H. M. Deng, J. Zhang, W.-J. Zheng, F. Paesani, and X.-B. Wang, J. Phys. Chem. Lett. **4**, 779 (2013).
[10] T. Kurtén, V. Loukonen, H. Vehkamäki, and M. Kulmala, Atmos. Chem. Phys. **8**, 4095 (2008).
[11] V. Loukonen, T. Kurtén, I. K. Ortega, H. Vehkamäki, A. A. H. Padua, K. Sellegri, and M. Kulmala, Atmos. Chem. Phys. **10**, 4961 (2010).
[12] J. Kirkby, J. Curtius, J. Almeida, E. Dunne, J. Duplissy, S. Ehrhart, A. Franchin, S. Gagné, L. Ickes, A. Kurten, A. Kupc, A. Metzger, F. Riccobono, L. Rondo, S. Schobesberger, G. Tsagkogeorgas, D. Wimmer, A. Amorim, F. Bianchi, M. Breitenlechner, A. David, J. Dommen, A. Downard, M. Ehn, R. C. Flagan, S. Haider, A. Hansel, D. Hauser, W. Jud, H. Junninen, F. Kreissl, A. Kvashin, A. Laaksonen, K. Lehtipalo, J. Lima, E. R. Lovejoy, V. Makhmutov, S. Mathot, J. Mikkilä, P. Minginette, S. Mogo, T. Nieminen, A. Onnela, P. Pereira, T. Petäjä, R. Schnitzhofer, J. H. Seinfeld, M. Sipilä, Y. Stozhkov, F. Stratmann, A. Tome, J. Vanhanen, Y. Viisanen, A. Vrtala, P. E. Wagner, H. Walther, E. Weingartner, H. Wex, P. M. Winkler, K. S. Carslaw, D. R. Worsnop, U. Baltensperger, and M. Kulmala, Nature (London) **476**, 429 (2011).
[13] M. Kulmala, J. Kontkanen, H. Junninen, K. Lehtipalo, H. E. Manninen, T. Nieminen, T. Petäjä, M. Sipilä, S. Schobesberger, P. Rantala, A. Franchin, T. Jokinen, E. Järvinen, M. Äijälä, J. Kangasluoma, J. Hakala, P. P. Aalto, P. Paasonen, J. Mikkilä, J. Vanhanen, J. Aalto, H. Hakola, U. Makkonen, T. Ruuskanen, R. L. Mauldin III, J. Duplissy, H. Vehkamäki, J. Bäck, A. Kortelainen, I. Riipinen, T. Kurtén, M. V. Johnston, J. N. Smith, M. Ehn, T. F. Mentel, K. E. J. Lehtinen, A. Laaksonen, V.-M. Kerminen, and D. R. Worsnop, Science **339**, 943 (2013).
[14] H. Junninen, M. Ehn, T. Petäjä, L. Luosujärvi, T. Kotiaho, R. Kostiainen, U. Rohner, M. Gonin, K. Fuhrer, M. Kulmala, and D. R. Worsnop, Atmos. Meas. Tech. **3**, 1039 (2010).
[15] T. Kurtén, T. Petäjä, J. Smith, I. K. Ortega, M. Sipilä, H. Junninen, M. Ehn, H. Vehkamäki, L. Mauldin, D. R. Worsnop, and M. Kulmala, Atmos. Chem. Phys. **11**, 3007 (2011).
[16] M. Kulmala, I. Riipinen, M. Sipilä, H. E. Manninen, T. Petäjä, H. Junninen, M. Dal Maso, G. Mordas, A. Mirme, M. Vana, A. Hirsikko, L. Laakso, R.

M. Harrison, I. Hanson, C. Leung, K. E. J. Lehtinen, and V.-M. Kerminen, Science **318**, 89 (2007).
[17]A. B. Nadykto, F. Yu, M. V. Jakovleva, J. Herb, and Y. Xu, Entropy **13**, 554 (2011).
[18]B. Temelso, T. E. Morrell, R. M. Shields, M. A. Allodi, E. K. Wood, K. N. Kirschner, T. C. Castonguay, K. A. Archer, and G. C. Shields, J. Phys. Chem. A **116**, 2209 (2012).
[19]H. R. Leverentz, J. I. Siepmann, D. G. Truhlar, V. Loukonen, and H. Vehkamäki, J. Phys. Chem. A **117**, 3819 (2013).
[20]G. K. Schenter, S. M. Kathmann, and B. C. Garrett, Phys. Rev. Lett. **82**, 3484 (1999).
[21]S. M. Kathmann, G. K. Schenter, and B. C. Garrett, J. Chem. Phys. **111**, 4688 (1999).
[22]F. Yu, J. Geophys. Res. D **111**, D01204, doi:10.1029/2005JD005968 (2006).
[23]F. Yu, Atmos. Chem. Phys. **6**, 5193 (2006).
[24]M. J. McGrath, T. Olenius, I. K. Ortega, V. Loukonen, P. Paasonen, T. Kurtén, M. Kulmala, and H. Vehkamäki, Atmos. Chem. Phys. **12**, 2345 (2012).
[25]I. K. Ortega, O. Kupiainen, T. Kurtén, T. Olenius, O. Wilkman, M. J. McGrath, V. Loukonen, and H. Vehkamäki, Atmos. Chem. Phys. **12**, 225 (2012).
[26]M. J. Frisch, G. W. Trucks, H. B. Schlegel *et al*., GAUSSIAN 09, Revision A.1, Gaussian, Inc., Wallingford, CT, 2009.
[27]A. D. Becke, J. Chem. Phys. **98**, 5648 (1993).
[28]J. A. Montgomery, Jr., M. J. Frisch, J. W. Ochterski, and G. A. Petersson, J. Chem. Phys. **110**, 2822 (1999).
[29]R. Ahlrichs, M. Bär, M. Häser, H. Horn, and C. Kölmel, Chem. Phys. Lett. **162**, 165 (1989).
[30]C. Hättig and F. Weigend, J. Chem. Phys. **113**, 5154 (2000).
[31]T. H. Dunning, Jr., K. A. Peterson, and A. K. Wilson, J. Chem. Phys. **114**, 9244 (2001).
[32]See supplementary material at http://dx.doi.org/10.1063/1.4819024 for the thermochemical data, dipole moments, and polarizabilities of the clusters included in the simulations.
[33]H. Vehkamäki, *Classical Nucleation Theory in Multicomponent Systems* (Springer-Verlag, Berlin, Germany, 2006).
[34]G. K. Yue and L. Y. Chan, J. Colloid Interface Sci. **68**, 501 (1979).
[35]B. R. Bzdek, J. W. DePalma, D. P. Ridge, J. Laskin, and M. V. Johnston, J. Am. Chem. Soc. **135**, 3276 (2013).
[36]T. Su and M. T. Bowers, J. Chem. Phys. **58**, 3027 (1973).
[37]O. Kupiainen, I. K. Ortega, T. Kurtén, and H. Vehkamäki, Atmos. Chem. Phys. **12**, 3591 (2012).
[38]H. Israël, *Atmospheric Electricity* (Israel Program for Sci. Transl. & NSF, Jerusalem, 1970), Vol. I.
[39]D. R. Bates, Planet. Space Sci. **30**, 1275 (1982).
[40]H. Berresheim, T. Elste, C. Plass-Dülmer, F. L. Eisele, and D. J. Tanner, Int. J. Mass Spectrom. **202**, 91 (2000).
[41]T. Petäjä, R. L. Mauldin III, E. Kosciuch, J. McGrath, T. Nieminen, P. Paasonen, M. Boy, A. Adamov, T. Kotiaho, and M. Kulmala, Atmos. Chem. Phys. **9**, 7435 (2009).
[42]H. E. Manninen, T. Nieminen, I. Riipinen, T. Yli-Juuti, S. Gagné, E. Asmi, P. P. Aalto, T. Petäjä, V.-M. Kerminen, and M. Kulmala, Atmos. Chem. Phys. **9**, 4077 (2009).
[43]H. E. Manninen, T. Petäjä, E. Asmi, I. Riipinen, T. Nieminen, J. Mikkilä, U. Hõrrak, A. Mirme, S. Mirme, L. Laakso, V.-M. Kerminen, and M. Kulmala, Boreal Environ. Res. **14**, 591 (2009).
[44]V.-M. Kerminen, T. Petäjä, H. E. Manninen, P. Paasonen, T. Nieminen, M. Sipilä, H. Junninen, M. Ehn, S. Gagné, L. Laakso, I. Riipinen, H. Vehkamäki, T. Kurtén, I. K. Ortega, M. Dal Maso, D. Brus, A. Hyvärinen, H. Lihavainen, J. Leppä, K. E. J. Lehtinen, A. Mirme, S. Mirme, U. Hõrrak, T. Berndt, F. Stratmann, W. Birmili, A. Wiedensohler, A. Metzger, J. Dommen, U. Baltensperger, A. Kiendler-Scharr, T. F. Mentel, J. Wildt, P. M. Winkler, P. E. Wagner, A. Petzold, A. Minikin, C. Plass-Dülmer, U. Pöschl, A. Laaksonen, and M. Kulmala, Atmos. Chem. Phys. **10**, 10829 (2010).
[45]I. Riipinen, S.-L. Sihto, M. Kulmala, F. Arnold, M. Dal Maso, W. Birmili, K. Saarnio, K. Teinilä, V.-M. Kerminen, A. Laaksonen, and K. E. J. Lehtinen, Atmos. Chem. Phys. **7**, 1899 (2007).
[46]X. Ge, A. S. Wexler, and S. L. Clegg, Atmos. Environ. **45**, 524 (2011).
[47]M. Dal Maso, A. Hyvärinen, M. Komppula, P. Tunved, V.-M. Kerminen, H. Lihavainen, Y. Viisanen, H.-C. Hansson, and M. Kulmala, Tellus, Ser. B **60**, 495 (2008).